

## AX<sub>3</sub> Spin System Dynamics from Forbidden Cross Peaks in Double-Quantum Two-Dimensional NMR Experiments, with Application to Acyl Carrier Protein

LEWIS E. KAY,\* T. A. HOLAK,† AND J. H. PRESTEGARD†

*Departments of \*Molecular Biophysics and Biochemistry and †Chemistry,  
Yale University, New Haven, Connecticut 06511*

Received March 24, 1987; revised June 4, 1987

A theoretical description of the origin of the several types of forbidden cross peaks encountered in two-dimensional double-quantum spectra of AX<sub>3</sub> spin systems in macromolecules is presented. We present a double-quantum data set for a small protein, acyl carrier protein (ACP), and focus on the seven alanine residues found in ACP. An analysis of the forbidden peaks associated with the alanine residues and threonine-2 indicates that the carboxyl terminus of the protein is much more flexible than the amino terminus. We discuss how an understanding of methyl group dynamics obtained from such spectra can aid in the correct interpretation of NOE cross peaks involving these groups in terms of internuclear distances. © 1988 Academic Press, Inc.

### INTRODUCTION

The internal motions of spin systems in macromolecules can be both a subject of interest and a potential stumbling block in the formulation of structural descriptions. Side chains in proteins, for example, must move for proteins to function, and the rates of these movements can be strongly correlated with kinetic mechanisms. Movement of side chains at rates which influence spin relaxation, however, prevents straightforward interpretation of cross-relaxation effects in terms of internuclear distances and structure. It would be very useful to identify a reliable indicator of internal motion in features observed in one or more of the standard two-dimensional NMR techniques used in the characterization of macromolecules so that motional effects could be properly analyzed.

Recently, Müller *et al.* (1-3) and Rance *et al.* (4) have reported the appearance of forbidden cross peaks in <sup>1</sup>H multiple-quantum-filtered correlation spectra and multiple-quantum spectra of proteins. These forbidden cross peaks arise from two distinct processes. They are either strong coupling effects (2) or differential transverse relaxation rates associated with transitions in degenerate spin systems (1-5). Here we focus our attention on cross peaks arising from the latter effect and the possibility that these can provide qualitative indicators of internal motion. More specifically, we will analyze forbidden peaks in 2D double-quantum spectra associated with an AX<sub>3</sub> spin system. These spin systems occur frequently in proteins as methyl- $\alpha$ -proton systems in alanine and the AX<sub>3</sub> portions of more complex spin systems found in threonine, valine, leucine, and isoleucine. Using coherence transfer selection rules developed by Ernst and co-

workers (6) it is easily shown that cross peaks from an  $AX_3$  spin system on the skew diagonal at  $(2\omega_X, \omega_X)$  and four-spin two-quantum cross peaks at  $(3\omega_X - \omega_A, \omega_X)$  should be eliminated in a double-quantum 2D NMR spectrum. They are, however, observed (1-5, 7) and we shall attempt to explain their presence. Our discussion follows closely our recent treatment of an  $A_3$  spin system (5). There we were able to extract some motional properties of  $A_3$  spin systems of micelles of deoxycholate from a profile of the forbidden double-quantum intensity obtained as a function of double-quantum excitation time. We also showed that the appearance of these forbidden peaks provides a sensitive probe of cross-correlation effects among spins, since, in the absence of such effects, degenerate transitions of  $A_nX_m$  spin systems will decay uniformly, and no forbidden peaks will be observed. We emphasize that violation of the extreme narrowing condition is in itself not a sufficient condition for the generation of forbidden peaks in multiple-quantum spectra. This result was derived explicitly for an  $A_3$  spin system in a previous publication (5).

As an illustration of the potential utility of forbidden cross peaks, we present data on  $AX_3$  spin systems in double-quantum-filtered 2D data sets for a small protein, acyl carrier protein (8) (ACP; 8847 Da). In particular we focus our attention on the seven alanine residues found in ACP. We also discuss how an understanding of methyl group dynamics can aid in the interpretation of NOE cross-peak intensities in terms of distances to be used in a structure determination.

#### THEORY

Figure 1 shows an energy level diagram and associated wavefunctions for an isolated  $AX_3$  spin system. Consider the double-quantum pulse sequence (9)

$$(90^\circ)_{\phi_1} - \tau - (180^\circ)_{\phi_1} - \tau - (90^\circ)_{\phi_1} - t_1 - (90^\circ)_{\phi_2} - t_2, \quad [1]$$

where  $\phi_1$  and  $\phi_2$  are phases of pulses cycled so as to eliminate all orders of coherence  $p$  except  $p = 2(2m + 1)$ ,  $m = 0, 1, 2, \dots$ . The effects of this sequence can be understood by using density matrix equations (10) in which the effects of relaxation have been included explicitly (10, 11). It is important to recognize that the choice of basis functions depicted in Fig. 1 ensures that magnetization from either of the  $I = \frac{3}{2}$  or  $I' = \frac{3}{2}$  manifolds is not mixed with magnetization from the  $I = \frac{1}{2}$  or  $I' = \frac{1}{2}$  manifolds upon application of RF pulses or during evolution due to chemical-shift and scalar-coupling effects. This greatly simplifies the calculations. However, relaxation does couple elements of magnetization associated with the  $I(I') = \frac{3}{2}$  manifolds with elements from the  $I(I') = \frac{1}{2}$  manifolds. Redfield theory (11) can be used to describe the coupling of transverse elements of the density matrix during the excitation period  $2\tau$  and during acquisition  $t_2$  as is illustrated in the following:

$$\begin{aligned} \frac{d}{dt} \rho_{78} &= R_{7878} \rho_{78} \\ \frac{d}{dt} \rho_{14} &= R_{1414} \rho_{14} \\ \frac{d}{dt} \rho_{47} &= R_{4747} \rho_{47} + R_{4726} \rho_{26} + R_{4735} \rho_{35}, \end{aligned} \quad [2]$$

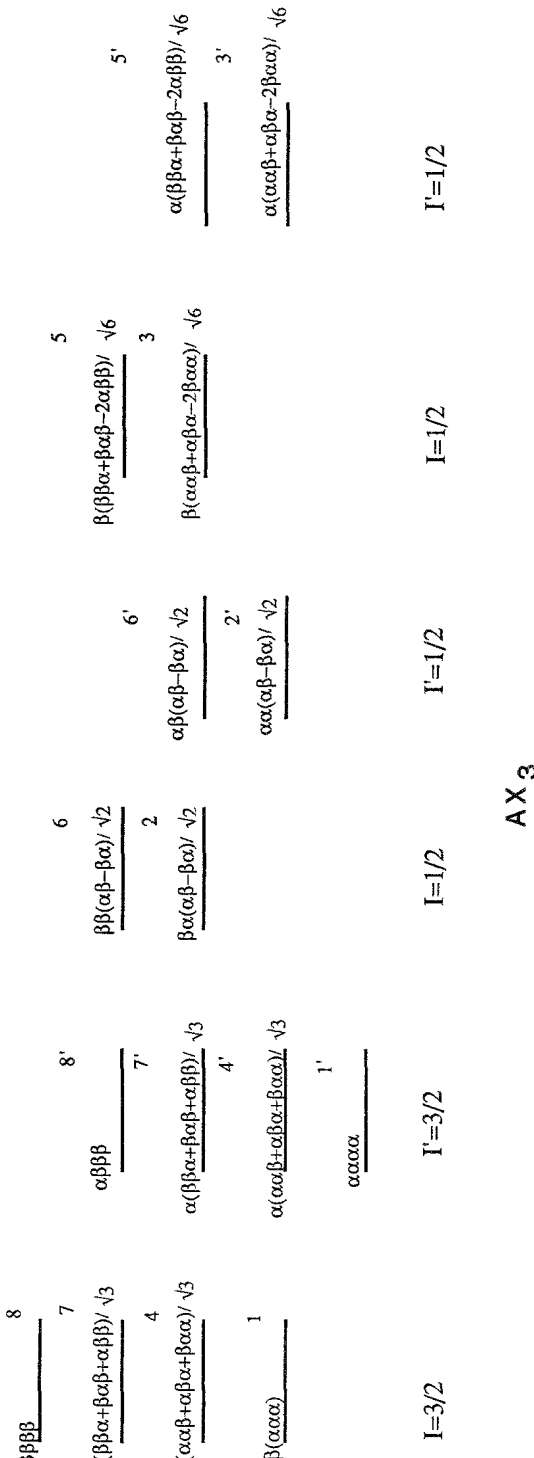


FIG. 1. Energy level diagram and associated wave functions for an  $AX_3$  spin system written in an irreducible basis representation.

where we have retained only those Redfield elements containing spectral density functions evaluated at  $\omega = 0$ . These are the most significant elements for macromolecules tumbling in the nonextreme narrowing regime. Inspection of Eq. [2] shows that the transverse relaxation of  $\rho_{14}$  and  $\rho_{78}$  is monoexponential and that the coupling is restricted to the transverse relaxation of  $\rho_{47}$ .

The Redfield elements of Eq. [2] characterizing this relaxation consist of linear combinations of spectral density functions that can be evaluated by considering an appropriate model for the dynamics of  $\text{AX}_3$  spin systems. We have modified the cone model of Brainard and Szabo (12) using the method of Hubbard (13) to yield expressions for the appropriate auto and cross-spectral density functions. The details are found in a previous publication (5). Briefly, the model employed has four parameters: an isotropic rotational correlation time,  $1/6D$ , a methyl group internal rotational correlation time,  $1/4D'$ , a methyl axis wobbling frequency,  $6D_w$ , and an order parameter,  $S_{\text{cone}}$ .  $S_{\text{cone}}$  can be defined according to

$$S_{\text{cone}} = 1/2 \cos \theta (1 + \cos \theta), \quad [3]$$

where  $\theta$  is the angle of the cone in which the methyl group wobbles.

When Redfield elements are written in terms of these parameters, the decay of  $\rho_{47}$  will in general remain nonexponential. There are, however, model specific conditions which can lead to a simplification of the expression for the evolution of  $\rho_{47}$  given in Eq. [2]. If the overall molecular tumbling time is slow compared to  $1/\omega$ , where  $\omega$  is the Larmor frequency, while the methyl internal motion is fast compared to both  $\omega$  and methyl wobbling (i.e.,  $S_{\text{cone}}^2 > 0.1$ ,  $4D' > 2D_w/(1 - S_{\text{cone}}^2)$ ,  $6D$ ,  $(\omega/6D) > 1$ , and  $(\omega/4D') < 1$ ) then we can ensure that

$$R_{4747} > R_{4726}, R_{4735}. \quad [4]$$

Hence, under these conditions, the transverse relaxation of  $\rho_{47}$  ( $\rho_{4'7'}$ ) can also be described by a single time constant. This time constant is, however, quite insensitive to overall tumbling of the molecule and is therefore much larger than that for  $\rho_{14}$  and  $\rho_{78}$  decay. We shall call the two time constants  $T_{2f}$  for  $\rho_{14}$  and  $\rho_{78}$  decay and  $T_{2s}$  for  $\rho_{47}$  decay. The motional restrictions necessary for this simplification are common in proteins, as illustrated by results from  $^{13}\text{C}$  relaxation studies of methyl groups of alanine in BPTI (14).

Evaluation of time constants,  $T_{2f}$  and  $T_{2s}$ , is best pursued through the analysis of forbidden peak intensities. Using methods outlined in a previous publication (5) it is readily shown that for the forbidden peaks on the skew diagonal ( $2\omega_X$ ,  $\omega_X$ ), the  $x$  component of magnetization after application of the pulse sequence given by Eq. [1] with  $\phi_1 = \phi_2 = \pi/2$  is given by

$$\begin{aligned} M_x \propto & \cos(2\pi J_{AX}\tau) [\exp(-2\tau/T_{2f}) - \exp(-2\tau/T_{2s})] \{ \cos(2\omega_X - 2\pi J_{AX})t_1 \\ & + \cos(2\omega_X + 2\pi J_{AX})t_1 \} \exp(-t_1/T_{2,2Q}) \{ \cos(\omega_X - \pi J_{AX})t_2 \\ & + \cos(\omega_X + \pi J_{AX})t_2 \} [\exp(-t_2/T_{2f}) - \exp(-t_2/T_{2s})]. \end{aligned} \quad [5]$$

In Eq. [5],  $\omega_X$  is the resonance frequency (in rad/s) of the methyl group where we have neglected second-order frequency shifts (15),  $J_{AX}$  is the  $\alpha\text{CH}-\beta\text{CH}_3$  coupling constant for the alanine  $\text{AX}_3$  spin system, and  $T_{2,2Q}$  is the transverse double-quantum relaxation

rate. A result similar to Eq. [5] has been derived for the response of a spin- $\frac{3}{2}$  system (e.g.,  $^{23}\text{Na}$ ) to a double-quantum filter (16, 17).

In an analogous fashion one can derive expressions for the forbidden cross peaks centered at  $(3\omega_X - \omega_A, \omega_X)$ . These peaks bear an analogy to combination lines appearing in one-dimensional experiments of strongly coupled spin systems (6) and present an alternate route for the determination of  $T_{2f}$  and  $T_{2s}$ . They are also observed by application of the pulse sequence given by Eq. [1] with  $\phi_1 = \phi_2 = \pi/2$ . A density matrix treatment of this pulse sequence retaining only those terms modulated at frequency  $(3\omega_X - \omega_A)$  in  $t_1$  shows that

$$M_X \propto 6f[\exp(-t_2/T_{2f}) - \exp(-t_2/T_{2s})]\{\sin(\omega_X - \pi J_{AX})t_2 - \sin(\omega_X + \pi J_{AX})t_2\}, \quad [6]$$

where  $f$  is a function dependent on evolution in the  $\tau$  and  $t_1$  domains and is given by

$$f = \cos(3\omega_X - \omega_A)t_1[\exp(-t_1/T'_{2,2Q})]\{6[\exp(-2\tau/T_{2f}) - \exp(-2\tau/T_{2s})]\sin 2\pi J_{AX}\tau + \exp(-2\tau/T_{2A})[3 \sin 2\pi J_{AX}\tau - \sin 6\pi J_{AX}\tau]\}. \quad [7]$$

In Eqs. [6] and [7]  $\omega_A$  is the first-order resonance frequency of the  $\alpha\text{CH}$  proton in the alanine spin system,  $T'_{2,2Q}$  is the transverse relaxation rate for the four-spin two-quantum transition resonating at  $3\omega_X - \omega_A$ , and  $T_{2A}$  is the transverse relaxation rate of the  $\alpha\text{CH}$  proton. Although lines of the  $\alpha$ -proton quartet (A spin) may in principle have different  $T_2$  values, we consider the limiting case where all four lines relax with the same time constant  $T_{2A}$  to simplify Eq. [7]. This assumption is borne out by experiment where all four components of the A resonance have similar linewidths.  $T_{2A}$  is thus an average measure of the interrelaxation of the A and  $X_3$  parts of the  $\text{AX}_3$  spin system.

Similarly, the expression for allowed magnetization centered at  $(3\omega_X - \omega_A, \omega_A)$  is

$$M_X \propto f[\exp(-t_2/T_{2A})]\{\sin(\omega_A - 3\pi J_{AX})t_2 - 3 \sin(\omega_A - \pi J_{AX})t_2 + 3 \sin(\omega_A + \pi J_{AX})t_2 - \sin(\omega_A + 3\pi J_{AX})t_2\} \quad [8]$$

with all the terms defined as in Eqs. [5], [6], and [7] and the constants of proportionality in Eqs. [6] and [8] the same. Comparing Eqs. [5], [6], and [8] to equations for normal double-quantum cross peaks at  $(\omega_A + \omega_X, \omega_A)$  and at  $(\omega_A + \omega_X, \omega_X)$ , it is clear that if normal cross peaks are phased to pure absorption then the cross peaks described in Eqs. [6] and [8] will be in the pure absorption mode while the forbidden peaks centered at  $(2\omega_X, \omega_X)$  will be in the dispersive mode in  $\omega_2$ . A slice through the center of the forbidden peaks described by either Eq. [5] or Eq. [6] parallel to  $\omega_2$  gives resonances at the frequencies  $\omega_X + \pi J_{AX}$  and  $\omega_X - \pi J_{AX}$ . For each frequency two Lorentzian lines with opposite phases and with linewidths of  $1/\pi T_{2f}$  and  $1/\pi T_{2s}$  are obtained. Hence, for data sets with sufficient resolution and  $S/N$  it should be possible to extract  $T_{2f}$  and  $T_{2s}$  from a fit of either of these lines to the expressions given by the Fourier transforms of Eq. [5] or [6]. For macromolecules tumbling isotropically in the non-extreme narrowing limit and with methyl group internal rotation satisfying the conditions described above, (i.e.,  $(\omega/6D) > 1$ ,  $S_{\text{cone}}^2 > 0.1$ ,  $4D' > 2D_w/(1 - S_{\text{cone}}^2)$ ,  $6D$ , and  $(\omega/4D') < 1$ ) it is possible to express  $-T_{2f}^{-1} = R_{7878} = R_{1414}$  and  $-T_{2s}^{-1} \sim R_{4747}$  in terms of just two parameters,  $S_{\text{cone}}$  and  $D_w$  (5). Thus, once accurate values for  $T_{2s}$  and  $T_{2f}$

are obtained an order parameter and time constant for wobble can be extracted. Figure 2 shows a theoretical lineshape of a forbidden peak defined by Eq. [6].

#### EXPERIMENTAL METHODS

The preparation and handling of ACP samples have been described previously (8). In our case a 15 mM sample dissolved in 55 mM potassium phosphate buffer ( $D_2O$ ) at pH 5.4 was used, and the data were recorded at 303 K. The double-quantum 2D experiment was carried out on a home-built 490 MHz spectrometer operating in the Fourier transform mode. A data set consisting of 590  $t_1$  experiments and 160 accumulations per experiment, each with 2K complex points, was recorded in the phase-sensitive mode using the method of States *et al.* (18). A relaxation delay of 0.75 s was used with an acquisition time of 0.38 s. Two dummy scans preceded each experiment to keep  $z$  magnetization near a steady-state value throughout the experiment. Spectral widths of 5.4 kHz in the  $\omega_2$  dimension and 10.8 kHz in  $\omega_1$  were employed with the carrier frequency placed on the residual water peak. The data were processed on a Vax 11/750 computer equipped with a CSPI Minimap array processor. Data were multiplied in both dimensions by exponential functions corresponding to a line broadening of 1 Hz to avoid lineshape distortions associated with functions giving better peak resolution. All files were zero-filled to 4K before Fourier transformation.

#### RESULTS AND DISCUSSION

A section of a double-quantum-filtered spectrum of ACP is shown in Fig. 3. Alanine methyl peaks are observed between 1.2 and 1.6 ppm and alanine  $\alpha$  peaks are observed between 4.1 and 4.6 ppm in a one-dimensional spectrum of the protein. Normal two-quantum peaks are observed in the lower half of Fig. 3 at  $(\omega_A + \omega_X, \omega_A)$  and  $(\omega_A + \omega_X, \omega_X)$ . A horizontal line connecting peaks for alanine-45 is shown, bisected by the skew diagonal. Forbidden peaks at  $(3\omega_X - \omega_A, \omega_X)$  and allowed peaks at  $(3\omega_X - \omega_A, \omega_A)$  for this residue are shown in the boxed regions of the upper half of the figure. The upper half of the plot is displayed with a lower contour level ( $\frac{1}{4}$  that of the

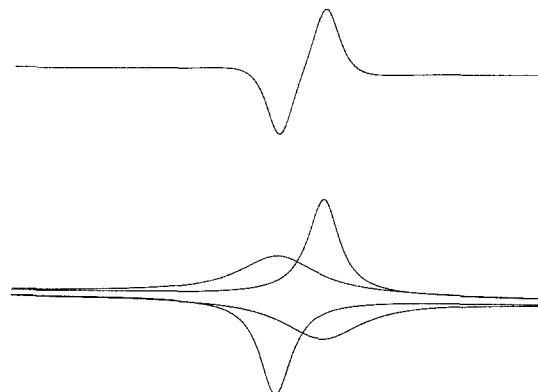


FIG. 2. The upper trace shows a theoretical lineshape of a cross section through a forbidden peak in the  $\omega_2$  dimension with  $1/\pi T_{2s} = 6$  Hz and  $1/\pi T_{2f} = 15$  Hz. The bottom trace illustrates the four components that contribute to the line (see Eq. [6]).

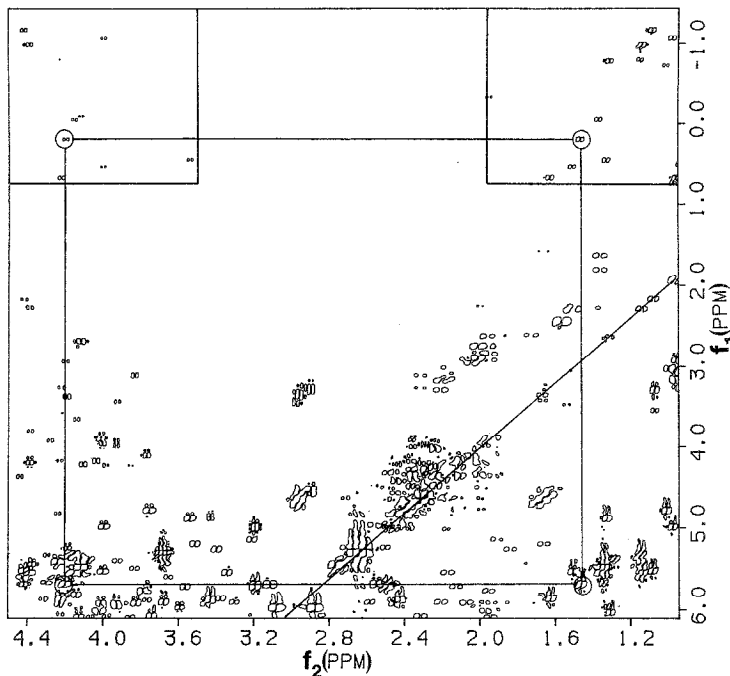


FIG. 3. A section of a double-quantum-filtered spectrum of ACP. A horizontal line connecting allowed cross peaks ( $(\omega_A + \omega_X, \omega_A)$  and  $(\omega_A + \omega_X, \omega_X)$ ) for alanine-45 is shown, bisected by the skew diagonal. Forbidden peaks at  $(3\omega_X - \omega_A, \omega_X)$  are indicated in the box on the upper right-hand side of the plot and allowed peaks at  $(3\omega_X - \omega_A, \omega_A)$  are shown in the upper left-hand side box. The upper half of the diagram is plotted with a lower contour level ( $\frac{1}{4}$  of the level of the lower half) to make peaks at  $\omega_1 = 3\omega_X - \omega_A$  more visible.

lower half) to make forbidden peaks more visible. Figures 4 and 5 show expanded plots of the boxed regions in Fig. 3.

While extraction of  $T_{2s}$  and  $T_{2f}$  from a fit of the lineshapes associated with cross peaks centered at  $(2\omega_X, \omega_X)$  or  $(3\omega_X - \omega_A, \omega_X)$  is possible for high-quality data sets, in practice we have found that only the cross peaks at  $(3\omega_X - \omega_A, \omega_X)$  are suitable for lineshape analysis. Our inability to use peaks centered at  $(2\omega_X, \omega_X)$  is due to the fact that the  $S/N$  of these forbidden peaks is poor since the intensity of these peaks depends on the differential relaxation rates of transitions 1-4 and 4-7 during both excitation and acquisition, unlike the intensity of forbidden peaks centered at  $(3\omega_X - \omega_A, \omega_X)$  which depends on differential relaxation during acquisition and only in part on differential relaxation during excitation. In addition, magnetization centered at  $(2\omega_X, \omega_X)$  is split into a doublet in the  $\omega_1$  dimension thereby halving the intensity of each multiplet component.

In a few cases cross sections of peaks centered at  $(3\omega_X - \omega_A, \omega_X)$  show the expected superposition of broad and narrow peaks as expected from Eq. [6]. An example is shown in Fig. 6. Quantitative fits of the shapes of these peaks would in principle yield values for  $S_{\text{cone}}$  and  $D_w$ . However, more qualitative analyses based on comparison of intensities of forbidden and allowed peaks can also be instructive.

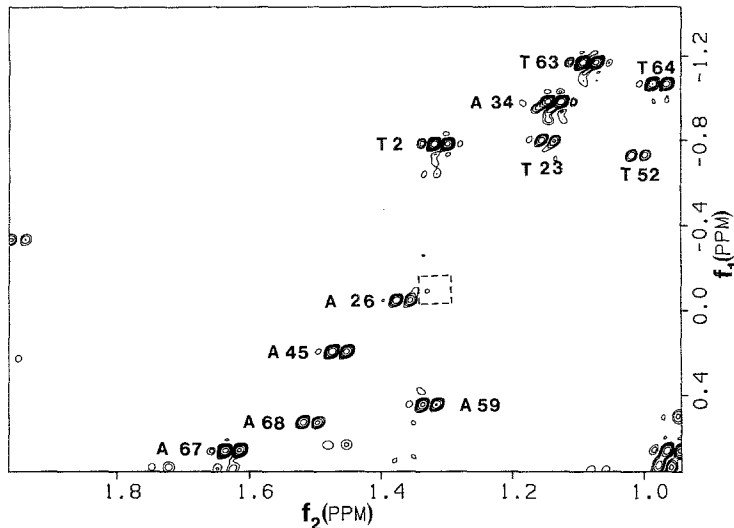


FIG. 4. Expanded plot of the  $(3\omega_X - \omega_A, \omega_X)$  region. The boxed region indicates where the peak from alanine-77 was expected.

Inspection of Eq. [6] shows that as  $T_{2s}$  approaches  $T_{2f}$  the forbidden peak centered at  $(3\omega_X - \omega_A, \omega_X)$  will disappear. This is a condition produced if internal motions lead to effective isotropic reorientation. Qualitative information concerning the magnitudes of  $T_{2s}$  and  $T_{2f}$  can thus be obtained by noting the simple appearance or absence of forbidden peaks.

Comparing the intensities of multiplet components of cross peaks centered at  $(3\omega_X - \omega_A, \omega_X)$  and  $(3\omega_X - \omega_A, \omega_A)$  in the limit of  $T_{2f} \ll T_{2s}$  provides a measure of  $T_{2s}$ .

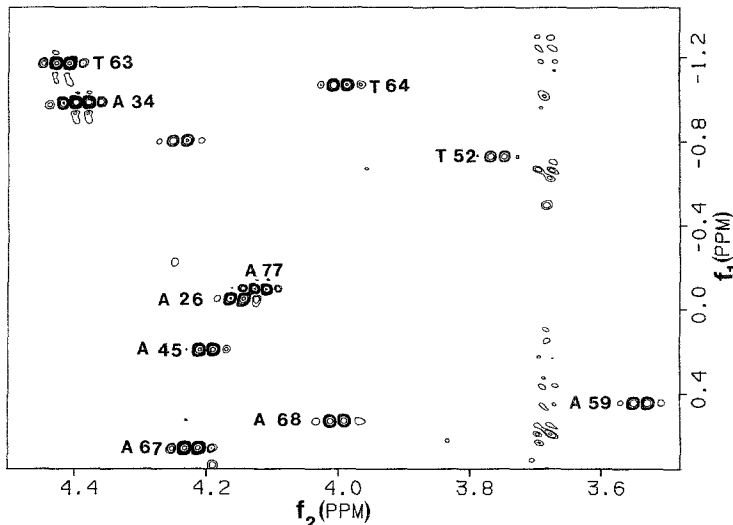


FIG. 5. Expanded plot of the  $(3\omega_X - \omega_A, \omega_A)$  region.

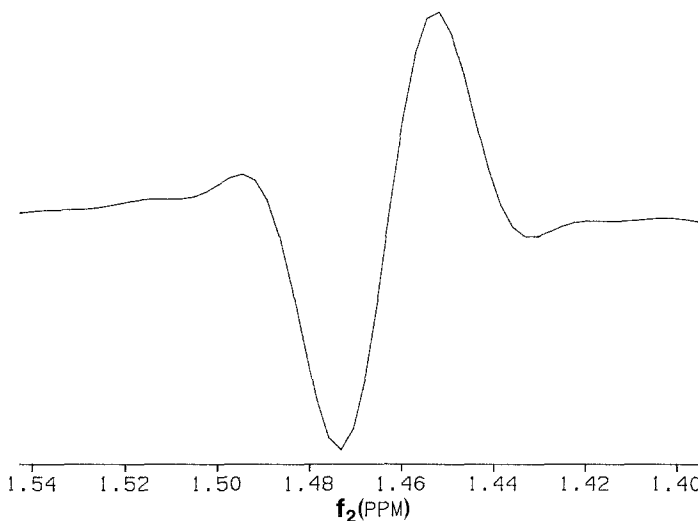


FIG. 6. Cross section parallel to  $\omega_2$  through the forbidden peak of alanine-45 centered at  $(3\omega_X - \omega_A, \omega_X)$ .

relative to  $T_{2A}$ . Table 1 contains a listing of the ratio of peaks at  $(3\omega_X - \omega_A, \omega_X \pm \pi J_{AX})$  and  $(3\omega_X - \omega_A, \omega_A \pm \pi J_{AX})$  for the alanine residues found in ACP. With the exception of Ala-77 for which no forbidden peak at  $(3\omega_X - \omega_A, \omega_X)$  is observed all the alanines give ratios of 2 to within the accuracy of the data. Inspection of Eqs. [6] and [8] shows that a ratio of 2 corresponds to  $T_{2A} = T_{2s} - T_{2f}$ , which in the limit  $T_{2f} \ll T_{2s}$  implies that  $T_{2A} \sim T_{2s}$ . The validity of the assumption that  $T_{2f} \ll T_{2s}$  was examined by fitting the forbidden lines to the Fourier transform of Eq. [6]. Best fits of the data gave  $T_{2f} \sim 0$ . The values of  $T_{2s}$  along with the values of  $T_{2A}$  obtained by fitting the lines

TABLE 1  
Intensity Ratios and Linewidths of Peaks Centered at  
 $(3\omega_X - \omega_A, \omega_X)$  and  $(3\omega_X - \omega_A, \omega_A)$

Ala	Intensity ratio <sup>a</sup>	$T_{2s}$ (ms) <sup>b</sup>	$T_{2A}$ (ms) <sup>c</sup>
26	1.6	45	47
34	2.0	44	51
45	2.5	41	45
59	2.3	44	42
67	2.0	40	43
68	1.9	39	40
77	0	—	56

<sup>a</sup> Intensity ratio of multiplet components centered at  $(3\omega_X - \omega_A, \omega_X - \pi J_{AX})$  and  $(3\omega_X - \omega_A, \omega_A + \pi J_{AX})$ .

<sup>b</sup> Measured from linewidth of multiplet centered at  $(3\omega_X - \omega_A, \omega_X - \pi J_{AX})$ .

<sup>c</sup> Measured from linewidth of multiplet centered at  $(3\omega_X - \omega_A, \omega_A + \pi J_{AX})$ .

centered at  $(3\omega_X - \omega_A, \omega_A)$  are presented in Table 1 and indicate that for all alanine residues, except Ala-77,  $T_{2A}, T_{2s} \gg T_{2f}$ . This is reasonable in a limit where dipolar interactions between the A and  $X_3$  parts of the  $AX_3$  spin system dominate  $T_{2s}$ .

The fact that no forbidden peak was observed for Ala-77 implies that for this particular case  $T_{2s} \sim T_{2f}$ . Such a result would occur if the  $AX_3$  spin system of Ala-77 executed isotropic motion characterized by a correlation time  $\tau_i$  such that  $\omega\tau_i < 1$ . Experimental verification of this suggestion can be found in the work of Müller *et al.* (1) and Rance *et al.* (4) which shows that forbidden peaks are not present in multiple-quantum-filtered spectra of individual amino acids. The absence of a forbidden peak implies that for Ala-77 Eq. [4] (i.e.,  $R_{4747} > R_{4726}, R_{4735}$ ) is no longer valid so that relaxation of  $\rho_{47}$  is coupled to the relaxation of  $\rho_{26}$  and  $\rho_{35}$ . This gives rise to uniform relaxation of all transverse elements in the  $\frac{3}{2}$  and  $\frac{1}{2}$  manifolds. In particular, this result emphasizes that cross-correlation effects between spins are necessary but not sufficient for the generation of forbidden peaks in multiple-quantum spectra. Thus, it appears that Ala-77, at the carboxyl terminus of the molecule, is very flexible. In contrast to Ala-77, an intense forbidden peak is observed for the  $AX_3$  portion of the spin system of Thr-2. This suggests that the amino terminus of the protein is much less flexible.

A qualitative indication of internal motion from a frequently applied 2D NMR experiment is of potential advantage in the analysis of macromolecular structure by 2D NMR. Structural analysis is currently based on interpretation of cross peaks in 2D NOE experiments in terms of internuclear distances. Despite internal motions, cross peaks involving methyl groups are potentially valuable because they are easily observed and assigned. While simple axial rotation can be easily accommodated in an analysis of the relaxation of methyl groups, there is always the possibility that the methyl group in question may execute more complex motions which may have to be described by order parameters much less than 1. If this were the case interpretation of NOE data pertaining to this methyl group in terms of rapid axial rotation and a simple  $1/r^6$  model would be incorrect and could lead to gross errors in distances. Alanine methyl groups having motional properties described by order parameters  $\ll 1$  and correlation times  $1/6D_w \ll 1/\omega$  can be easily recognized since they will have greatly reduced forbidden multiple-quantum peak intensities relative to other alanine residues. NOE data from alanine residues displaying a reduced or negligible forbidden peak intensity should be excluded from a structure determination unless some rigorous account of the complicated dynamics is taken into account.

More quantitative descriptions of methyl group motions are in principle possible using lineshapes of forbidden cross peaks. The opposite phase of the superimposed lines allows a rather simple and accurate extraction of  $T_{2s}$  and  $T_{2f}$  without complex time evolution experiments. We have not attempted to do this here because an  $AX_3$  model is really an oversimplification of the spin systems of alanine residues in ACP. In particular, we know that a description of the relaxation of alanine  $AX_3$  spin systems in proteins involves neighboring spins. It is these very relaxation interactions that give rise to NOE data useful in structural analysis. Qualitatively these contributions tend to make  $T_{2f}$  very small, while having a much less significant effect on  $T_{2s}$ . These differential effects, when combined with other information such as the magnitude of NOE cross peaks, may allow a more quantitative separation of internal motion effects from remote spin effects. Nevertheless, at present we feel that the simple identification

of groups with substantial internal motion, and elimination of data involving these groups from structural analysis, is adequate justification for pursuit of experiments such as those described.

#### ACKNOWLEDGMENTS

This work was supported by Grants GM-32243 and GM-33225 from the National Institutes of Health and by a predoctoral fellowship to L.E.K. from the Natural Sciences and Engineering Research Council of Canada. The research benefited from instrumentation provided through shared instrumentation programs of the National Institute of General Medical Science, GM 32243S1, and the Division of Research Resources of NIH, RR02379. We thank Dr. D. Hare for writing the 2D NMR processing, display, and plotting routines.

*Note added in proof.* A more detailed account of the material presented herein will appear in a paper by N. Müller, G. Bodenhausen, and R. R. Ernst, *J. Magn. Reson.*, in press.

#### REFERENCES

1. N. MÜLLER, G. BODENHAUSEN, K., WÜTHRICH, AND R. R. ERNST, *J. Magn. Reson.* **65**, 531 (1985).
2. N. MÜLLER, R. R. ERNST, AND K. WÜTHRICH, *J. Am. Chem. Soc.* **108**, 6482 (1986).
3. N. MÜLLER, *Chem. Phys. Lett.* **131**, 218 (1986).
4. M. RANCE AND P. E. WRIGHT, *Chem. Phys. Lett.* **124**, 572 (1986).
5. L. E. KAY AND J. H. PRESTEGARD, *J. Am. Chem. Soc.* **109**, 3829 (1987).
6. L. BRAUNSCHWEILER, G. BODENHAUSEN, AND R. R. ERNST, *Mol. Phys.* **48**, 533 (1986).
7. C. DALVIT, M. RANCE, AND P. E. WRIGHT, *J. Magn. Reson.* **69**, 356 (1986).
8. T. A. HOLAK AND J. H. PRESTEGARD, *Biochemistry* **25**, 5766 (1986).
9. A. BAX, "Two-Dimensional Nuclear Magnetic Resonance in Liquids," Delft Univ. Press, Dordrecht, 1982.
10. C. P. SLICHTER, "Principles of Magnetic Resonance," 2nd ed., Springer, Berlin, 1978.
11. A. G. REDFIELD, in "Advances in Magnetic Resonance" (J. S. Waugh, Ed.), Vol. 1, p. 1, Academic Press, New York, 1965.
12. J. R. BRAINARD AND A. SZABO, *Biochemistry* **20**, 4618 (1981).
13. J. R. HUBBARD, *J. Chem. Phys.* **52**, 563 (1970).
14. R. RICHARZ, K. NAGAYAMA, AND K. WÜTHRICH, *Biochemistry* **19**, 5189 (1980).
15. L. G. WERBELOW, *J. Magn. Reson.* **34**, 439 (1979).
16. J. PEKAR AND J. S. LEIGH, *J. Magn. Reson.* **69**, 582 (1986).
17. G. JACCARD, S. WIMPERIS, AND G. BODENHAUSEN, *J. Chem. Phys.* **85**, 11 (1986).
18. D. J. STATES, R. A. HABERKORN, AND D. J. REUBEN, *J. Magn. Reson.* **48**, 286 (1982).